Probabilities for Radiative and Nonradiative Decay of Er^{3+} in LaF_3†

M. J. WEBER

Raytheon Research Division, Waltham, Massachusetts

(Received 1 December 1966)

The rates of radiative and nonradiative decay were determined for several excited states of Er^{3+} in LaF_3 from calculated spontaneous emission probabilities and measured lifetimes. Electric-dipole, magnetic-dipole, and electric-quadrupole transition probabilities were evaluated using intermediate coupled states derived from computer diagonalization of the combined spin-orbit and electrostatic energy matrix. The required spin-orbit and Racah parameters for LaF_3: Er^{3+} were obtained from a least-squares fit of experimental and theoretical energy levels. The probabilities for electric-dipole transitions were calculated using the theory of Judd and Ofelt; the phenomenological parameters needed in this approach were derived from measurements of integrated absorption coefficients. By comparing the total calculated radiative lifetimes and the observed lifetimes, the probabilities for nonradiative decay from nine different excited states were determined. The probability of nonradiative decay was found to be very dependent upon the proximity of lower energy levels, which for the levels investigated ranged from approximately 1600 to 6000 cm^{-1}, and hence upon the number of phonons required to conserve energy. The rates of nonradiative transitions corresponding to the simultaneous emission of as many as five phonons were found to make significant contributions to the lifetimes of fluorescent states of rare earths in LaF_3.

INTRODUCTION

In a previous paper[1] (henceforth referred to as I), the fluorescence excitation and decay properties of Er^{3+} in LaF_3 were investigated to determine the modes of radiative and nonradiative decay and the excited-state lifetimes. The present study is addressed to the problem of determining the magnitudes of the various radiative and nonradiative processes active for the relaxation of specific energy levels and, thereby, the quantum efficiencies for emission.

An excited paramagnetic ion impurity in a crystal may relax by a combination of radiative processes, including purely electronic and phonon-assisted transitions of various multipole nature, and nonradiative processes, such as phonon emission and resonant energy transfer arising from ion-ion coupling. In this investigation, we shall be interested principally in determining the rates of nonradiative decay by multiple phonon emission. Since these processes are not directly observable, their presence and relative importance are established by comparing the measured excited-state lifetime with the total radiative lifetime, any difference being attributed to the existence of nonradiative transitions. Relaxation caused by ion-ion interactions is not considered; in obtaining the experimental results reported in I, these processes were deliberately avoided by using low rare-earth concentrations.

The radiative lifetime of a state can be found (1) by calculating the total spontaneous emission probability or (2) from combined measurements of relative and absolute intensities in absorption and fluorescence spectra.[2] The first approach is used here since it is also of interest to establish the success with which one can calculate radiative transition probabilities for the rare earths. The probabilities for magnetic-dipole and electric-quadrupole transitions between states of the ground $4f^N$ configuration of trivalent rare earths can be readily calculated.[3] Electric-dipole transitions, on the other hand, require an admixing of states of opposite parity from higher configurations into $4f^N$ and, at present, *ab initio* calculations are not possible. Judd[4] and Ofelt[5] have shown, however, that under certain simplifying assumptions the probabilities for electric-dipole transitions can be expressed as of sum of a small number of terms involving parameters which contain the strength of the configuration mixing. These parameters have been evaluated from absolute intensity measurements of the optical spectra; attempts to calculate the experimentally determined parameters have thus far met with difficulties. This theory, which has been discussed by several authors and applied to explain the observed spectral intensities of rare-earth ions in liquids[4,6] and solids[7–10] with reasonable, albeit qualified, success, is utilized in the present study.

† Research supported in part by U.S. Army Engineering Research and Development Laboratory, Fort Belvoir, Virginia, under Contract No. DA 44-009-AMC-743(T).

[1] M. J. Weber, Phys. Rev. **156**, 231 (1967).

[2] K. H. Hellwege, Naturwiss. **34**, 212 (1947). The application of the second approach has recently been illustrated for the $^4S_{3/2} \rightarrow {}^4I_{15/2}$ transition of Er^{3+} in yttrium gallium garnet by J. R. Chamberlain, D. H. Paxman, and J. L. Page, Proc. Phys. Soc. (London) **89**, 143 (1966).

[3] See, for example, B. G. Wybourne, *Spectroscopic Properties of Rare Earths* (John Wiley & Sons, Inc., New York, 1965).

[4] B. R. Judd, Phys. Rev. **127**, 750 (1962).

[5] G. S. Ofelt, J. Chem. Phys. **37**, 511 (1962).

[6] W. T. Carnall, P. R. Fields, and B. G. Wybourne, J. Chem. Phys. **42**, 3797 (1965).

[7] J. D. Axe, Jr., J. Chem. Phys. **39**, 1154 (1963).

[8] W. F. Krupke and J. B. Gruber, Phys. Rev. **139**, A2008 (1965).

[9] W. F. Krupke, Phys. Rev. **145**, 325 (1966).

[10] M. J. Weber, in Proceedings of the Johns Hopkins Conference on Optical Properties of Ions in Crystals (to be published).

Spontaneous emission probabilities were calculated using intermediate coupled states obtained by fitting the energy levels from the observed spectra of Er^+ in LaF_3.

Relaxation within a J multiplet of the rare-earth ion in a crystal is generally rapid because the energy-level separations are usually within the frequency spectrum of lattice vibrations and hence one- and two-phonon relaxation processes[11] are very probable. These nonradiative processes cause lifetime broadening of lines in optical spectra[12] and are active for spin-lattice relaxation as studied in microwave resonance experiments.[13] We shall not be concerned with this relaxation which, as discussed in I, brings about a rapid thermal equilibration within a crystal-field multiplet, but rather the relaxation between different multiplets by multiple phonon emission. Since intermultiplet separations for the rare earths typically range from several hundred to several thousand cm^{-1} whereas the maximum lattice phonon energies in crystals may only be a few hundred cm^{-1}, several phonons are required to conserve energy in large, purely nonradiative transitions. The rates of these processes are, accordingly, sensitive to the proximity of neighboring energy levels. This is reflected in the variation of excited-state lifetimes with energy gap to the next-lower level as found, for example, by Barasch and Dieke[14] and in I. Calculations of the probability of decay by multiphonon emission are nontrivial, however, since a complete treatment combines elements of both crystal-field theory and lattice dynamics. Kiel[15] has indicated how these transitions can be treated using high-order time-dependent perturbation theory and pointed out that the probabilities for successively higher-order phonon processes may be expected to decrease much more slowly than in the analogous photon case because of the greater density of modes and stronger coupling. This appears to be borne out, in a semiquantitative fashion, from the explicit study of ten excited J states of Er^{3+} in LaF_3.

EIGENSTATES FOR Er^{3+} IN LaF_3

Transitions between individual Stark levels of rare-earth ions in crystals are usually resolvable in low-temperature optical spectra and therefore eigenstates of an ion in the crystalline field are needed to calculate the associated transition probabilities. Unfortunately, one is stymied in this pursuit of LaF_3 because (1) the rare-earth site symmetry is not definitely established (proposed symmetries[16–25] include C_{2v}, C_2, C_s and D_{3h}, C_{3v}, or small deviations therefrom) and (2), for a lattice site having low symmetry, many parameters are needed to describe the crystalline field and a truly meaningful determination of their values requires sufficient information to identify levels properly and a careful study of the convergence of any parameter-fitting procedure.[26] We therefore content ourselves throughout this paper with consideration of total transition probabilities between crystal-field multiplets obtained using essentially "free-ion" states. The line strength for a transition arising from a tensor operator $T_q^{(k)}$ will thus involve a summation over magnetic quantum number J_z and polarization given by[27]

$$S(\alpha J;\alpha' J') = \sum_{J_z J_z' q} |\langle \alpha J J_z | T_q^{(k)} | \alpha' J' J_z' \rangle|^2 = |\langle \alpha J || \mathbf{T}^{(k)} || \alpha' J' \rangle|^2, \quad (1)$$

where J is the total angular momentum and α denotes all other quantum numbers. Implicit in the application of Eq. (1) to crystal-field spectra is that all levels of the initial J multiplet are equally populated. Also, the transition frequency will be a mean for allowed transitions between all levels of the initial and final multiplets.

The eigenstates of Er^{3+} in intermediate coupling were found by diagonalization of the combined spin-orbit and electrostatic energy matrix. The required spin-orbit parameter ζ and the Racah parameters E^1, E^2, and E^3 were first determined by an iterative fitting procedure in which the centers of gravity of twenty-one crystal-field multiplets of LaF_3:Er^{3+}, as measured by Krupke and Gruber[28] (KG), were compared with theoretical levels calculated using estimated parameters. Differences between the experimental and theoretical eigenvalues were minimized with a computer program which made successive adjustments of each parameter to improve an over-all least-squares fit.

[11] R. Orbach, Proc. Roy. Soc. (London) **A264**, 458 (1961).
[12] S. Yatsiv, Physica **28**, 521 (1962).
[13] M. B. Schulz and C. D. Jeffries, Phys. Rev. **149**, 270 (1966) have studied spin-lattice relaxation of several rare earths in LaF_3.
[14] G. E. Barasch and G. H. Dieke, J. Chem. Phys. **43**, 988 (1965).
[15] A. Kiel, in *Quantum Electronics*, edited by P. Grivet and N. Bloembergen (Columbia University Press, New York, 1964), p. 765.
[16] I. Oftedal, Z. Physik. Chem. (Frankfurt) **6**, 272 (1929); **13**, 190 (1931).
[17] K. Schlyter, Arkiv Kemi **5**, 73 (1953).
[18] D. A. Jones, J. M. Baker, and D. F. D. Pope, Proc. Phys. Soc. (London) **74**, 249 (1959).
[19] J. M. Baker and R. S. Rubins, Proc. Phys. Soc. (London) **78**, 1353 (1961).
[20] E. Y. Wong, O. M. Stafsudd, and D. R. Johnston, Phys. Rev. **131**, 990 (1963); J. Chem. Phys. **39**, 786 (1963).
[21] W. F. Krupke and J. B. Gruber, J. Chem. Phys. **39**, 1024 (1963).
[22] V. M. Mansmann, Z. Anorg. Allgem. Chem. **331**, 98 (1964).
[23] H. H. Caspers, R. A. Buchanan, and H. R. Marlin, J. Chem. Phys. **41**, 94 (1964).
[24] A. Zalkin, D. H. Templeton, and T. E. Hopkins (to be published).
[25] L. O. Andersson and W. G. Proctor, Z. Krist. (to be published).
[26] See, for example, the discussion in Ref. 13, p. 288.
[27] A. R. Edmonds, *Angular Momentum in Quantum Mechanics* (Princeton University Press, Princeton, New Jersey, 1957), p. 76.
[28] W. F. Krupke and J. B. Gruber, J. Chem. Phys. **39**, 1024 (1963); **41**, 1225 (1964); **42**, 1134 (1965).

TABLE I. Energies and eigenvectors of intermediate coupled states for Er^{3+} in LaF_3.

	Energy (cm^{-1})	Eigenvector						
$J=1/2$		^2P	^4D					
	33 336	−0.9579	0.2871					
	46 808	0.2871	0.9579					
$J=3/2$		^2P	$^2D(20)$	$^2D(21)$	^4S	^4D	^4F	
	18 320	−0.4196	−0.2666	−0.0207	0.8371	0.0415	0.2237	
	22 227	0.0702	0.4486	−0.0039	0.3918	0.0016	−0.8002	
	31 477	0.6049	0.4720	0.1832	0.3380	−0.1770	0.4819	
	42 044	−0.2973	0.5350	−0.1577	−0.0819	0.7335	0.2360	
	42 802	−0.5855	0.3991	0.4949	−0.1557	−0.4693	0.0928	
	54 910	−0.1482	0.2437	−0.8344	−0.0252	−0.4568	0.1144	
$J=5/2$		$^2D(20)$	$^2D(21)$	$^2F(10)$	$^2F(21)$	^4D	^4F	^4G
	21 870	−0.3483	0.1284	0.0402	0.0708	−0.0442	0.9232	−0.0370
	33 178	0.1071	0.0836	0.1507	0.1808	−0.0135	−0.0308	−0.9618
	34 641	−0.7688	0.3789	−0.0195	0.0266	−0.3626	−0.3627	−0.0340
	38 526	−0.5153	−0.4894	−0.0326	−0.0852	0.6797	−0.0910	−0.1276
	48 873	−0.0757	−0.6866	−0.1905	−0.2868	−0.6159	0.0619	−0.1452
	62 909	0.0642	0.3488	−0.4035	−0.8076	0.1525	0.0553	−0.1815
	93 134	−0.0255	−0.0186	0.8804	−0.4689	−0.0419	−0.0096	0.0462
$J=7/2$		$^2F(10)$	$^2F(21)$	$^2G(20)$	$^2G(21)$	^4D	^4F	^4G
	20 213	0.0449	0.0542	0.2096	−0.1545	0.0111	0.9624	0.0294
	27 877	0.1380	0.1439	−0.5140	0.4848	0.0560	0.1943	−0.6482
	33 783	0.0442	0.0329	0.5270	−0.3883	0.0354	−0.1589	−0.7362
	39 067	0.1544	0.0912	0.0319	−0.0087	0.9780	−0.0349	0.0954
	55 055	0.5830	0.7551	0.1369	0.0320	−0.1859	−0.0972	0.1619
	64 688	−0.0280	0.1772	−0.6227	−0.7606	0.0055	0.0060	−0.0394
	96 726	−0.7826	0.6044	0.0817	0.1040	0.0668	0.0010	−0.0133
$J=9/2$		$^2G(20)$	$^2G(21)$	$^2H(11)$	$^2H(21)$	^4F	^4G	^4I
	12 241	0.2765	−0.2204	0.1953	−0.4125	0.3611	0.0116	−0.7322
	15 076	0.2882	−0.2158	−0.0012	0.0838	0.7725	0.0883	0.5087
	24 322	0.4397	−0.3920	0.2706	−0.4032	−0.4862	0.2450	0.3475
	27 305	−0.0126	0.0545	0.0997	−0.3806	0.0209	−0.8916	0.2161
	36 268	0.4900	−0.3945	−0.3011	0.5617	−0.1879	−0.3552	−0.1912
	46 989	−0.0835	−0.1601	−0.8744	−0.4401	0.0007	0.0896	0.0332
	68 765	0.6323	0.7530	−0.1532	−0.0784	−0.0257	0.0537	0.0036
$J=11/2$		$^2H(11)$	$^2H(21)$	^2I	^4G	^4I		
	10 022	−0.1073	0.3740	0.0631	0.1094	0.9125		
	19 175	0.1500	−0.6908	−0.0570	−0.5962	0.3762		
	26 327	0.3306	−0.5117	−0.0209	0.7771	0.1569		
	40 164	0.5473	0.1337	0.8173	−0.1161	−0.0330		
	50 061	−0.7464	−0.3212	0.5695	0.1235	−0.0102		
$J=13/2$		^2I	^2K	^4I				
	6 405	−0.0319	0.0896	−0.9955				
	32 392	0.3149	0.9461	0.0751				
	42 797	−0.9486	0.3111	0.0584				
$J=15/2$		^2K	^2L	^4I				
	0	−0.1708	−0.0176	0.9852				
	27 176	0.9548	0.2440	0.1698				
	46 667	−0.2434	0.9696	−0.0249				
$J=17/2$		^2L						
	40 508	1.0000						

The parameter values, after ten complete iterations, were

$$\zeta = 2345\ \text{cm}^{-1}, \qquad E^1 = 6747\ \text{cm}^{-1},$$
$$E^2 = 31.63\ \text{cm}^{-1}, \qquad E^3 = 635.8\ \text{cm}^{-1}.$$

These values compare favorably with those reported by KG. The resulting eigenstates are linear combinations of basis states $|\, 4f^N \alpha SLJ \rangle$ of the form

$$|\, \psi_J \langle = \sum_{\alpha SL} C(\alpha SL)\ |\, 4f^N \alpha SLJ \rangle. \qquad (2)$$

These states will henceforth be denoted by $|\, 4f^N [\alpha SL] J \rangle$, where the αSL labeling, in accordance with KG, will be that of the LS-coupled state to which each inter-

mediate coupled state reduces as the spin-orbit parameter is decreased to zero. The eigenvalues with respect to the $^4I_{15/2}$ ground state and the intermediate coupling coefficients $C(\alpha SL)$ in Eq. (2) computed from the above parameters are given in Table I. In cases where the same SLJ are derived from different Racah terms $(WUSL)$, the required U labels are added in parentheses.

Although only states within the $4f^{11}$ configuration of Er^{3+} were included above, Rajnak[29] has reported that, using the original KG level assignment, no further improvement in the fit was obtained upon the introduction of terms describing possible configuration interactions. An improvement was found, however, when the multiplet assigned to $^4G_{5/2}$ was changed to $^2K_{13/2}$. All crystal-field levels expected for $^2K_{13/2}$ have not been observed. In the above fit, the level at 32 992.2 cm^{-1} was assigned to $^4G_{5/2}$.

ELECTRIC-DIPOLE TRANSITIONS

Electric-dipole transitions require a change in parity between initial and final states and therefore are forbidden between $4f^N$ states of the rare earths. If the ion resides in a noncentrosymmetric static or dynamic crystal field, however, odd harmonics in the expansion of the crystalline potential can introduce a small admixture of opposite parity states from a higher configuration, such as $4f^{N-1}5d$, into the original $4f^N$ states and thereby electric-dipole transitions become allowed. Explicit calculations of the related probabilities would be very difficult because of the large number of states involved, most of whose energies are undetermined, and lack of knowledge of the strengths of the pertinent crystal-field parameters. To circumvent these difficulties and to render the problem more tractable, Judd[4] and Ofelt[5] have shown that by ascribing an average energy to all levels of a higher configuration $nf^{N-1}n'l'$, the oscillator strength of a transition between two multiplets can be simplified into a sum of products of phenomenological parameters T_λ and matrix elements of unit tensor operators $\mathbf{U}^{(\lambda)}$ of the form

$$f_{ed}=\frac{\nu}{2J+1}\sum_{\text{even}} T_\lambda \times\langle 4f^N[\alpha SL]J \,||\, \mathbf{U}^{(\lambda)} \,||\, 4f^N[\alpha' S'L']J'\rangle^2, \quad (3)$$

where ν is a mean frequency for the transition. The selection rules for electric-dipole transitions arising from configuration mixing include

$$\Delta l=\pm 1, \qquad \Delta S=0, \qquad |\Delta L|, |\Delta J| \leq 2l. \quad (4)$$

Neglecting crystal-field mixing of different multiplets, J is a good quantum number and for $4f^N$ ions, $|\Delta L|$, $|\Delta J| \leq 6$. In addition, terms of order λ in Eq. (3) and the initial and final J values must satisfy a triangle rule

$$|J-J'| \leq \lambda \leq |J+J'|. \quad (5)$$

[29] K. Rajnak, J. Chem. Phys. **43**, 847 (1965).

The matrix elements of $\mathbf{U}^{(\lambda)}$ can be evaluated from the formula

$$\langle f^N\alpha SLJ \,||\, \mathbf{U}^{(\lambda)} \,||\, f^N\alpha' S'L'J'\rangle = (-1)^{S+L'+J+\lambda}\delta(S,S')[(2J+1)(2J'+1)]^{1/2} \times \begin{Bmatrix} J & J' & \lambda \\ L' & L & S \end{Bmatrix} \langle f^N\alpha SL \,||\, \mathbf{U}^{(\lambda)} \,||\, f^N\alpha' S'L'\rangle. \quad (6)$$

Using the tabulated 6-j symbols,[30] $\{\ \}$, and doubly reduced matrix elements[31] for f^{11}, the $\mathbf{U}^{(\lambda)}$ matrix elements between intermediate coupled states of Er^{3+} in LaF_3 were calculated for most absorptive and emissive transitions of interest; the results are given in Table II.

The oscillator strength, and therefrom the parameters T_λ in Eq. (3), can be derived from measurements of the integrated absorption spectrum via the relationship[32]

$$f=\frac{mc}{\pi e^2 N}\int \mu d\nu, \quad (7)$$

where μ is the absorption coefficient (cm^{-1}) and N is the total number of active ions per unit volume. When the ion is embedded in a medium of refractive index n, the right-hand side of Eq. (7) must include a multiplicative factor of the form $n(E_0/E_{\text{eff}})^2$, where E_0 is an average field in the medium and E_{eff} is the field at the ion site effective in inducing transitions. These correction factors for electric- and magnetic-dipole transitions are usually approximated[32] by $9n/(n^2+2)^2$ and $1/n$, respectively; because they only differ by $\approx 10\%$ for LaF_3, no attempt was made to distinguish their separate contributions for the absorption strength in the few cases where they may be of comparable magnitude. Also, since the variation of n over the spectral region of interest is less than 5%,[33] we shall assume a constant correction factor and include it in the definition of T_λ.

Absorption spectra for Er^{3+} in LaF_3 were recorded at liquid-helium and liquid-nitrogen temperatures for frequencies up to $\approx 27\,000$ cm^{-1}. A modified Perkin–Elmer model 13G spectrometer was used as a single-beam, single-pass monochromator with the sample placed in an external optical system located at the exit. The sample was cooled by conduction in a double Dewar; with liquid helium, actual sample temperatures were in the range 6–10°K. Measurements were made of sample crystals containing 0.095 and 0.42 wt.% Er as

[30] M. Rotenberg, R. Bivens, N. Metropolis, and J. K. Wooten, Jr., *The 3-j and 6-j Symbols* (Technology Press, M.I.T., Cambridge, Massachusetts, 1959).

[31] C. W. Nielsen and G. F. Koster, *Spectroscopic Coefficients for the p^n, d^n, and f^n Configurations* (The M.I.T. Press, Cambridge, Massachusetts, 1963).

[32] See, for example, D. L. Dexter, in *Solid State Physics*, edited by F. Seitz and D. Turnbull (Academic Press Inc., New York, 1958), Vol. 6, p. 360.

[33] G. Haas, R. B. Ramsey, and R. Thun, J. Opt. Soc. Am. **49**, 116 (1959).

TABLE II. Reduced matrix elements of $\mathbf{U}^{(\lambda)}$ between intermediate coupled states of Er^{3+} in LaF_3.

$[SL]J$	$[S'L']J'$	$[\mathbf{U}^{(2)}]^2$	$[\mathbf{U}^{(4)}]^2$	$[\mathbf{U}^{(6)}]^2$
$^4I_{13/2}$	$^4I_{15/2}$	0.0188	0.1176	1.4617
$^4I_{11/2}$	$^4I_{15/2}$	0.0259	0.0001	0.3994
	$^4I_{13/2}$	0.021	0.11	1.04
$^4I_{9/2}$	$^4I_{15/2}$	0.0	0.1452	0.0064
	$^4I_{13/2}$	0.0003	0.0081	0.64
$^4F_{9/2}$	$^4I_{15/2}$	0.0	0.5655	0.4651
	$^4I_{13/2}$	0.0096	0.1576	0.0870
	$^4I_{11/2}$	0.0671	0.0088	1.2611
	$^4I_{9/2}$	0.096	0.0061	0.012
$^4S_{3/2}$	$^4I_{15/2}$	0.0	0.0	0.2285
	$^4I_{13/2}$	0.0	0.0	0.3481
	$^4I_{11/2}$	0.0	0.0037	0.0789
	$^4I_{9/2}$	0.0	0.0729	0.2560
$^2H_{11/2}$	$^4I_{15/2}$	0.7056	0.4109	0.0870
$^4F_{7/2}$	$^4I_{15/2}$	0.0	0.1467	0.6273
$^4F_{5/2}$	$^4I_{15/2}$	0.0	0.0	0.2237
$^4F_{3/2}$	$^4I_{15/2}$	0.0	0.0	0.1204
$^2H_{9/2}$	$^4I_{15/2}$	0.0	0.078	0.17
	$^4I_{13/2}$	0.073	0.12	0.41
	$^4I_{11/2}$	0.077	0.11	0.096
	$^4I_{9/2}$	0.0076	0.0050	0.0028
	$^4F_{9/2}$	0.010	0.030	0.059
$^4G_{11/2}$	$^4I_{15/2}$	0.9178	0.5271	0.1197
	$^4I_{13/2}$	0.1011	0.2642	0.2550
	$^4I_{11/2}$	0.0002	0.493	0.0144
	$^4I_{9/2}$	0.0645	0.0117	0.0467
	$^4F_{9/2}$	0.4436	0.0388	0.0104
	$^2H_{11/2}$	0.0006	0.16	0.11
$^2P_{3/2}$	$^4I_{15/2}$	0.0	0.0	0.026
	$^4I_{13/2}$	0.0	0.0	0.16
	$^4I_{11/2}$	0.0	0.13	0.025
	$^4I_{9/2}$	0.0	0.044	0.0092
	$^4F_{9/2}$	0.0	0.056	0.0045
	$^4S_{3/2}$	0.0847	0.0	0.0
$^4G_{9/2}$	$^4I_{15/2}$	0.0	0.0511	0.0002
$^4D_{5/2}$	$^4I_{15/2}$	0.0	0.0	0.020
	$^4I_{13/2}$	0.0	0.27	0.0002
	$^4I_{11/2}$	0.0	0.20	0.0042
	$^4I_{9/2}$	0.0479	0.0092	0.0236
	$^4F_{9/2}$	0.2411	0.36	~0
	$^4S_{3/2}$	0.032	0.0190	0.0
	$^2H_{11/2}$	0.0	0.0064	0.012
	$^4F_{7/2}$	0.10	0.10	~0
	$^4F_{5/2}$	0.20	0.029	0.0
	$^4F_{3/2}$	0.14	0.14	0.0
	$^2H_{9/2}$	0.078	0.0004	~0
	$^2P_{1/2}$	0.0900	0.0	0.0

determined by spectrochemical analysis; sample thicknesses were ~5–8 mm. The frequencies and oscillator strengths, from Eq. (7), at liquid-helium temperatures are tabulated in Table III. The spectra were in general agreement with those reported previously by Krupke

TABLE III. Frequencies and oscillator strengths of transitions observed in the absorption spectrum of LaF_3:Er^{3+} at liquid-helium temperatures. (An asterisk denotes unresolved structure.)

	Frequency (cm^{-1})	Oscillator strength
$^4I_{13/2}$	6 607	9.7×10^{-8}
	6 633	5.9
	6 672	9.4
	6 710	6.2
	6 724	27.3
	6 757	4.0
	6 825	4.7
$^4I_{11/2}$	10 303	2.4
	10 310	2.5
	10 329	3.2
	10 347	9.3
	10 363	1.0
	10 399	5.8
$^4I_{9/2}$	12 376	5.5
	12 395	8.1
	12 417	4.1
	12 847	5.9
	12 876	7.3
	12 912	6.5
	12 950	11.6
$^4F_{9/2}$	15 400	8.1
	15 438, 15 450	32.7
	15 483	7.4
	15 535	9.3
$^4S_{3/2}$	18 564	17.4
	18 594	16.0
$^2H_{11/2}$	19 271	11.2
	19 315, 19 318	31.4
	19 365*	31.0
	19 423	92.9
$^4F_{7/2}$	20 660	15.2
	20 707	11.3
	20 738	11.1
$^4F_{5/2}$	22 377*	11.0
	22 411	10.4
$^4F_{3/2}$	22 693	21.8
	22 755	12.2
$^2H_{9/2}$	24 610	6.7
	24 690	4.2
	24 761	4.1
	24 844	2.2
	24 865	5.0
$^4G_{11/2}$	26 504	1.3
	26 533	13.0
	26 562	19.1
	26 589	44.2
	26 654	55.6
	26 717	198.0

and Gruber[28] with the exception of the group of transitions to $^4I_{9/2}$. Of the lines reported by KG, only their most intense one at 12 420 cm^{-1} was observed; the origin of the other lines grouped under $^4I_{9/2}$ in Table III was not established. One impurity known to be present in the samples was Pr^{3+}; however, it has no absorption lines in the region 12 000–13 000 cm^{-1}.

The T_λ's found from Table III and Eqs. (3) and (7) are dependent upon which transitions are considered. In general, one may seek a set of T_λ's which will yield the best over-all fit to all measured oscillator strengths, however, examination of the double-bar matrix elements in Table II reveals that the relative importance of different terms for specific transitions varies greatly. Therefore, a weighted average may, in some cases, be preferable to a straightforward least-squares determination of T_λ. The neglect of J-state mixing of closely-spaced multiplets by the crystal field may also affect the results.

With the present data, the most probable source of error in evaluating T_λ is the use of oscillator strengths measured for transitions from only a few of the lower levels of $^4I_{15/2}$ to approximate an average of transitions from all crystal-field levels of an equally populated multiplet, as implied by the application of Eq. (1). That transitions from different levels of a multiplet are not all equally probable is evident from relative intensities of lines in absorption and fluorescence spectra. Because of the large crystal-field splitting of $^4I_{15/2}$ (443 cm^{-1}) and the line broadening which occurs at elevated temperatures, it was impractical to attempt to thermally populate all levels equally. The total oscillator strengths from $^4I_{15/2}$ to several multiplets were measured at both liquid-helium and liquid-nitrogen temperatures; the values differed, but the differences were always less than a factor of 2. While consideration of several $[\alpha SL]J \rightarrow [\alpha' S' L']J'$ transitions may tend to average out this effect and the neglect of J mixing, the attendant uncertainty in the determination of the T_λ's persists and accordingly the following best estimates must be accepted with reservations:

$$T_2 = 3.9\times10^{-20} \text{ sec},$$

$$T_4 = 1.0\times10^{-20} \text{ sec},$$

$$T_6 = 2.3\times10^{-20} \text{ sec}.$$

Since there are no absorption lines below 27 000 cm^{-1} for which $\Delta J = 0$, it was not possible to determine T_0, assuming it is allowed by the site symmetry.[34]

The rms deviation of the observed f numbers and those calculated from the above T_λ values is 0.2×10^{-6}. The oscillator strengths of the transitions studied range over almost two orders of magnitude; the deviation for the *average* oscillator strength is $\sim$25%. This agreement is generally as satisfactory as that found previously by Krupke[9] for Pr^{3+} and Nd^{3+} in LaF_3. The T_λ's are predicted to vary from ion to ion. The T_2 value for Er^{3+}, in particular, appears to be very much larger than that determined[35] for Pr^{3+} or Nd^{3+}.

SPONTANEOUS EMISSION PROBABILITIES

The probability for spontaneous emission is related to the associated oscillator strength by

$$A([\alpha SL]J; [\alpha' S' L']J') = (8\pi^2 e^2 n^2 \nu^2/mc^3) f([\alpha SL]J; [\alpha' S' L']J'), \tag{8}$$

and therefore, from Eq. (3),

$$A_{ed}([\alpha SL]J; [\alpha' S' L']J') = [8\pi^2 e^2 n^2 \nu^3/mc^3(2J+1)] \sum_{\lambda \text{ even}} T_\lambda \langle 4f^N[\alpha SL]J \,||\, \mathbf{U}^{(\lambda)} \,||\, 4f^N[\alpha' S' L']J' \rangle^2. \tag{9}$$

In Eqs. (8)–(9), f and T_λ are assumed to include allowance for the local field in the surrounding medium. If, as in the present case, the T's are determined from absorption data, then Eq. (9) is strictly applicable only if any deviation of the relationship between the Einstein A and B coefficients for optical emission and absorption probabilities is small for isolated rare-earth impurities.[36] Also, implicit in the $(2J+1)$ degeneracy factor in Eq. (9) is the assumption that all levels of the initial J multiplet are equally populated or that transitions from all crystal-field levels of the multiplet are equally probable.

Using the above values for T_λ and the matrix elements in Table II, $A_{ed}([\alpha SL]J; [\alpha' S' L']J')$ were calculated for transitions from all fluorescent levels and are tabulated in Table IV. Since the dipolar spontaneous emission probability decreases as ν^3, only the higher-frequency transitions were considered.

A T_0 term may contribute to the oscillator strengths for several of the radiative transitions. Because the magnitude of T_0 is unknown, the importance of this contribution remains undetermined. For Eu^{3+} in LaF_3, however, T_0 was found[10] to be very small,[37] $<2.0\times10^{-22}$ sec.

[34] This term appears only for sites having C_s, C_n, or C_{nv} point-group symmetries.
[35] Krupke's Ω_λ parameters (Ref. 9) and the present T_λ's are related by $T_\lambda = (8\pi^2 m/3h)[(n^2+2)^2/9n]\Omega_\lambda$.
[36] For a discussion of cases where this relationship ceases to be valid, see W. B. Fowler and D. L. Dexter, J. Chem. Phys. **43**, 1768 (1965) and references therein to earlier work.
[37] This would be consistent with an approximate D_{3h} site symmetry.

MAGNETIC-DIPOLE TRANSITIONS

Magnetic-dipole transitions are parity allowed between states of f^N and subject to selection rules $\Delta\alpha=\Delta S=\Delta L=0$, $\Delta J=0, \pm1(0\not\leftrightarrow0)$ in the Russel-Saunders limit. The probability for spontaneous emission of magnetic-dipole radiation between intermediate coupled states is given by

$$A_{\rm md}(J;\,J')=(2J+1)^{-1}(64\pi^4\nu^3n^3/3hc^3)\,|\sum_{\alpha SL,\,\alpha'S'L'}C(\alpha SL)C(\alpha'S'L')\,\langle 4f^N[\alpha SL]J\,||\,\mathbf{M}\,||\,4f^N[\alpha'S'L']J'\rangle\,|^2, \tag{10}$$

where the magnetic-dipole operator

$$\mathbf{M}=(-e/2mc)\sum_i(\mathbf{l}_i+g\mathbf{s}_i)=(-e/2mc)(\mathbf{L}+2\mathbf{S}). \tag{11}$$

The matrix elements of $\mathbf{M}$ between SLJ states are:

$J'=J$

$$(f^N\alpha SLJ\,||\,\mathbf{M}\,||\,f^N\alpha'S'L'J)=\delta(\alpha,\alpha')\delta(S,S')\delta(L,L')\beta[(2J+1)/4J(J+1)]^{1/2}\times[S(S+1)-L(L+1)+3J(J+1)], \tag{12a}$$

$J'=J-1$

$$\langle f^N\alpha SLJ\,||\,\mathbf{M}\,||\,f^N\alpha'S'L'J-1\rangle=\delta(\alpha,\alpha')\delta(S,S')\delta(L,L')\beta\left\{\frac{[(S+L+1)^2-J^2][J^2-(L-S)^2]}{4J}\right\}^{1/2}, \tag{12b}$$

$J'=J+1$

$$\langle f^N\alpha SLJ\,||\,\mathbf{M}\,||\,f^N\alpha'S'L'J+1\rangle=\delta(\alpha,\alpha')\delta(S,S')\delta(L,L')\beta\left\{\frac{[(S+L+1)^2-(J+1)^2][(J+1)^2-(L-S)^2]}{4(J+1)}\right\}^{1/2}, \tag{12c}$$

where $\beta=eh/2mc$.

The probabilities for all allowed magnetic-dipole transitions from fluorescent levels of Er^{3+} in LaF_3 were calculated using Eqs. (10)–(12) and the intermediate coupling coefficients in Table I; the results are tabulated in the fourth column of Table IV. Whereas magnetic-dipole emission makes a significant contribution to the radiative decay of the two lowest levels, $[^4I_{13/2}]$ and $[^4I_{11/2}]$, it accounts for only a small fraction ($\lesssim5\%$) of the total emission from the other fluorescent levels. The comments made previously regarding the assumption of equal population of all crystal-field levels of the initial J multiplet and the neglect of J-state mixing are again apropos.

ELECTRIC-QUADRUPOLE TRANSITIONS

Electric-quadrupole transitions are also parity allowed between states of f^N with the selection rules $\Delta S=0$, $|\Delta L|, |\Delta J|\leq2$. The oscillator strengths may be written,[38] in analogy to Eq. (3), as

$$f_{\rm eq}=\nu^3T_2'\langle f^N\alpha SLJ\,||\,\mathbf{U}^{(2)}\,||\,f^N\alpha'S'L'J'\rangle^2/(2J+1), \tag{13}$$

where

$$T_2'=\tfrac{1}{2}\tfrac{1}{2}\tfrac{2}{5}(\pi^3/\alpha)(a_0/c)^3\chi\langle f^N\,|\,r^2/a_0^2\,|\,f^N\rangle^2. \tag{14}$$

In Eq. (14), α is the fine-structure constant, a_0 is the Bohr radius, and χ is the local field correction $n(E_{\rm eff}/E_0)^2$ which is usually approximated by $n(n^2+2)^2/9$. Quadrupolar oscillator strengths were calculated using χ, $\langle r^2\rangle$ (from Freeman and Watson[39]), and $\mathbf{U}^{(2)}$ matrix elements appropriate for Er^{3+} in LaF_3. For a transition such as $^4I_{15/2}\rightarrow{}^4G_{11/2}$ which has both a large frequency[40] and $\mathbf{U}^{(2)}$ matrix element, $f_{\rm eq}=5.6\times10^{-10}$. This is more than three orders of magnitude smaller than the measured value and therefore unless some enhancement mechanism is operative, electric-quadrupole transitions can be considered to be unimportant for radiative decay.

The intensities of the $^4I_{15/2}\rightarrow{}^2H_{11/2}$ and $^4I_{15/2}\rightarrow{}^4G_{11/2}$ transitions of Er^{3+} have been recognized to be very sensitive to changes in the ligands. Jørgensen and Judd,[38] noting that these and other hypersensitive transitions obeyed $\Delta J=2$ quadrupolar-type selection rules, examined several possible ways in which the above oscillator strength might be increased. In particular, if an asymmetric distribution of dipoles is

[38] C. K. Jørgensen and B. R. Judd, Mol. Phys. **8**, 281 (1964).
[39] A. J. Freeman and R. E. Watson, Phys. Rev. **127**, 2058 (1962).
[40] Note that the spontaneous emission rate for electric-quadrupole radiation is proportional to ν^5.

TABLE IV. Predicted probabilities for spontaneous emission of electric- and magnetic-dipole radiation in $LaF_3:Er^{3+}$.

Transition	Average frequency (cm^{-1})	Probability electric-dipole emission (sec^{-1})	Probability magnetic-dipole emission (sec^{-1})	Total radiative lifetime (msec)	Observed lifetime (msec)
$^4I_{13/2}\rightarrow{}^4I_{15/2}$	6 481	54	37.6	10.9	13
$^4I_{11/2}\rightarrow{}^4I_{15/2}$	10 123	70	...	11.6	11
$^4I_{13/2}$	3 642	7.7	8.4		
$^4I_{9/2}\rightarrow{}^4I_{15/2}$	12 351	24	...		
$^4I_{13/2}$	5 870	23	...	20.7	~0.15
$^4I_{11/2}$	2 228		1.2		
$^4F_{9/2}\rightarrow{}^4I_{15/2}$	15 236	468	...		
$^4I_{13/2}$	8 755	23	...		
$^4I_{11/2}$	5 113	33	5.9	1.87	0.75
$^4I_{9/2}$	2 885	1	2.6		
$^4S_{3/2}\rightarrow{}^4I_{15/2}$	18 353	662	...		
$^4I_{13/2}$	11 872	268	...		
$^4I_{11/2}$	8 230	20	...	1.02	1.0
$^4I_{9/2}$	6 003	28	...		
$^2H_{11/2}\rightarrow{}^4I_{15/2}$	19 118	1220	...		
$^4I_{13/2}$	12 637		63.4		
$^4I_{11/2}$	8 994		94.8		<0.005
$^4I_{9/2}$	6 767		≈0		
$^4F_{9/2}$	3 882		0.2		
$^2H_{9/2}\rightarrow{}^4I_{15/2}$	24 527	570	...		
$^4I_{13/2}$	18 046	645	...		
$^4I_{11/2}$	14 404	152	36.2	0.682	0.095
$^4I_{9/2}$	12 176	7	1.0		
$^4F_{9/2}$	9 291	13	42.4		
$^2H_{11/2}$	5 409		1.0		
$^4F_{7/2}$	4 035		0.8		
$^4G_{11/2}\rightarrow{}^4I_{15/2}$	26 368	5530	...		
$^4I_{13/2}$	19 888	667	44.1		
$^4I_{11/2}$	16 245	24	0.1	0.153	~0.003
$^4I_{9/2}$	14 018	69	0.7		
$^4F_{9/2}$	11 133	165	3.0		
$^2H_{11/2}$	7 251	10	11.9		
$^2H_{9/2}$	1 842		0.1		
$^2P_{3/2}\rightarrow{}^4I_{15/2}$	31 501	338	...		
$^4I_{13/2}$	25 020	1180	...		
$^4I_{11/2}$	21 378	370	...		
$^4I_{9/2}$	19 150	78	...	0.43	0.29
$^4F_{9/2}$	16 265	66	...		
$^4S_{3/2}$	13 148	151	22.7		
$^4F_{5/2}$	9 339		29.7		
$^4F_{3/2}$	9 007		32.1		
$^4D_{5/2}\rightarrow{}^4I_{15/2}$	36 610	151	...		
$^4I_{13/2}$	32 129	1200	...		
$^4I_{11/2}$	28 487	669	...		
$^4I_{9/2}$	26 259	620	...		
$^4F_{9/2}$	23 374	2270	...		
$^4S_{3/2}$	20 257	163	8.6		
$^2H_{11/2}$	19 492	34	...		
$^4F_{7/2}$	18 118	387	9.4	0.153	0.020
$^4F_{5/2}$	16 448	487	0.3		
$^4F_{3/2}$	16 116	377	1.2		
$^2H_{9/2}$	14 083	114	...		
$^2G_{7/2}$	10 528		1.7		
$^2P_{3/2}$	7 109		6.2		
$^4G_{5/2}$	5 688		0.8		
$^2P_{1/2}$	5 190	17	...		
$^4G_{7/2}$	4 615		0.3		
$^2D_{5/2}$	3 772		0.1		

induced by the electromagnetic field in the vicinity of the rare-earth ion, this may greatly enhance the electric-field gradient and thereby the probability for electric-quadrupole transitions. It has since been realized[41] that first-order harmonics in the crystalline potential combined with the electric-dipole operator yield terms involving $\mathbf{U}^{(2)}$ which also obey quadrupolar selection rules. Thus this mechanism, which is included in Eq. (3) and is allowed for C_n, C_{nv}, and C_s site-group symmetries, may be the origin of the observed hypersensitivity. Note that for Er^{3+} the above transitions and the intense radiative transition $^4D_{5/2}\rightarrow{}^4F_{9/2}$ (see I) involve the largest $\mathbf{U}^{(2)}$ matrix elements in Table II.

NONRADIATIVE TRANSITIONS

The lifetime of an excited state i is governed by a combination of probabilities for all possible radiative and nonradiative transitions. If $W_{ij}{}^{\mathrm{R}}$ denotes the probability for radiative decay from state i to state j and W^{NR} that for the corresponding nonradiative decay, then

$$\tau_i{}^{-1}=\sum_j W_{ij}{}^{\mathrm{R}}+\sum_j W_{ij}{}^{\mathrm{NR}}, \tag{15}$$

where the summation is over all terminal states j. Given the lifetime τ_i, the rate of nonradiative transitions can be determined if the total radiative probability $\sum W_{ij}{}^{\mathrm{R}}$ or, alternatively, the quantum efficiency is known, the latter quantity being defined by

$$\eta_i=\sum_j W_{ij}{}^{\mathrm{R}}/(\sum_j W_{ij}{}^{\mathrm{R}}+\sum_j W_{ij}{}^{\mathrm{NR}})=\tau_i\sum_j W_{ij}{}^{\mathrm{R}}. \tag{16}$$

The total calculated radiative lifetimes and the measured lifetimes[1] of fluorescent levels of $LaF_3:Er^{3+}$ are compared in the final two columns of Table IV.

As noted in I, there is a definite trend throughout the energy-level scheme of $LaF_3:Er^{3+}$ that the smaller the energy gap to the next-lower J multiplet, the shorter the lifetime. This is illustrated in Fig. 1 where the total decay probability $1/\tau$ of several levels is plotted as a function of the minimum energy gap to the next-lower multiplet. Also plotted are the total radiative probabilities from Table IV. In general, for levels having energy gaps $\gtrsim 3000$ cm^{-1}, the observed and radiative lifetimes do not differ greatly and thus the quantum efficiencies are near unity. For levels with energy gaps <3000 cm^{-1}, the discrepancies between the radiative and observed decay probabilities are larger, indicative of the increased importance of nonradiative processes. Finally, for energy gaps <1600 cm^{-1}, nonradiative decay is so dominant that fluorescence is normally not detected.

Nonradiative decay between J multiplets is attributed[42] to phonon emission arising from interactions of the orbital moment of the ion with the fluctuating crystalline field caused by lattice vibrations. Since the fundamental lattice phonon frequencies of LaF_3, as derived from infrared and Raman spectra[43] and vibrational sidebands,[44] only range up to 350–400 cm^{-1}, the simultaneous emission of several phonons is required to conserve energy in a purely nonradiative transition. Kiel[15] has shown one way in which such processes can occur by extending the Kronig–Van Vleck treatment[45] of the orbit-lattice coupling in spin-lattice relaxation theory to multiphonon emission using higher-order time-dependent perturbation theory. To minimize the number of phonons required, and hence the order of the process, the highest-energy optical phonon branches are considered to be most significant for relaxation. Explicit calculations of the probabilities for spontaneous emission of several phonons are hampered, however, because very little is known about the strength of the orbit-lattice coupling; also, they are tedious because many different vibrational modes and combinations of intermediate states may need to be considered. Although information above the orbit-lattice interaction can be derived from data on temperature-dependent line shifts and linewidths in optical spectra, lifetime broadening, and spin-lattice relaxation, the important contributions for these processes may arise from phonons having different frequencies and corresponding to different vibrational modes from those important for multiphonon emission. A detailed discussion of the theory of multiphonon processes and

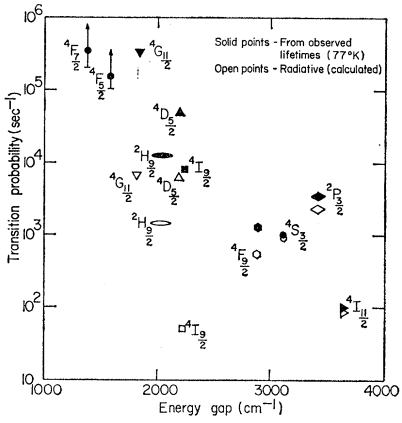

FIG. 1. Radiative and measured decay probabilities for excited states of Er^{3+} in LaF_3 plotted as a function of energy gap to the next-lower multiplet.

[41] B. R. Judd, J. Chem. Phys. **44**, 839 (1966).

[42] Nonradiative decay arising from energy transfer to other Er^{3+} ions or impurities is assumed to make a negligibly small contribution to the lifetimes measured in Ref. 1.

[43] H. H. Caspers, R. A. Buchanan, and H. R. Marlin, J. Chem. Phys. **41**, 94 (1964).

[44] W. M. Yen, W. C. Scott, and A. L. Schawlow, Phys. Rev. **136**, A271 (1964).

[45] R. deL. Kronig, Physica **6**, 33 (1939); J. H. Van Vleck, Phys. Rev. **57**, 426 (1940).

calculations of their rates will be presented elsewhere; in this paper we are concerned principally with the experimental determination of their rates and dependence on the size of the transition energy.

The probabilities for nonradiative decay W^{NR} from several levels were determined from the results in I and Table IV and are plotted in Fig. 2, again as a function of the energy gap to the next-lower multiplet. The values shown for $^4F_{5/2}$ and $^4F_{7/2}$ are from the observed lifetimes which, because the relative fluorescence intensities from these levels were extremely weak, were assumed to be governed predominantly by nonradiative decay. The accuracies of the total nonradiative probabilities and quantum efficiencies found from Eqs. (15) and (16) are naturally dependent upon the experimental uncertainties associated with the lifetime measurements, which are known, and the effects of the approximations made in calculating the radiative probabilities, the latter being more difficult to appraise (the error bars in Fig. 2 are thus lower limits). For large energy gaps where the radiative and observed lifetimes are comparable, the probable errors for W^{NR} are accordingly large.[46] Also, in the case of $^2P_{3/2}$ and $^4D_{5/2}$, the radiative lifetime may be shorter because several low-frequency transitions were not considered.

In spite of the above uncertainties, a distinct and dramatic change in the rate of nonradiative decay with size of energy gap is clearly evident. Over the energy range studied, an increase in energy gap by two results in a decrease in decay rate of 3–4 orders of magnitude. Kiel attempted to estimate the amount by which the multiphonon emission probability would decrease as the energy gap, and therefore the number of phonons required, was increased and concluded that in favorable cases the ratio of probabilities for n- and $(n+1)$-phonon processes may be ~ 20 or smaller. The results in Fig. 2 are in surprisingly good, albeit a bit fortuitous, agreement with this rough prediction. A single such number, however, is not expected to be adequate over a wide energy range and for different eigenstates.[47]

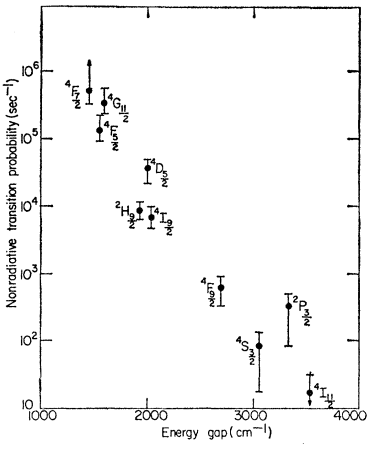

FIG. 2. Nonradiative transition probabilities at 77°K for several excited states of Er^{3+} in LaF_3 plotted as a function of energy gap to the next-lower multiplet.

It is perhaps tempting to draw a smooth curve through the data points in Fig. 2 and use it to predict the rate of nonradiative decay from other energy levels of Er^{3+} and different rare-earth ions, however, it must be remembered that the number and relative importance of different vibrational modes active for relaxation are dependent upon the character of the states involved. Which modes are allowed to connect electronic states of interest can be determined group theoretically from the symmetry properties of the vibrations at the ion site. Also, if the orbit-lattice interaction is expressed as a combination of spherical harmonic components, then terms containing operators of degree λ must satisfy a triangle rule[48] of the type given in Eq. (5). Whereas this is not a severe restriction on the possible nonradiative transitions between most adjacent J multiplets of Er^{3+}, it is for excited $^5D_J(J=0, 1, 2, 3)$ multiplets of Eu^{3+} in LaF_3. The nonradiative decay rates for the latter[10] are much slower than expected from Fig. 2 for comparable energy gaps since several important terms are forbidden.

If one remains cognizant of possible selection-rule restrictions, the results in Figs. 1 and 2 do provide qualitative guidance for predicting from which levels of rare-earth ions in LaF_3 fluorescence might normally be observed. To my knowledge, the importance of a minimum energy gap of $\gtrsim 1600$ cm^{-1} for normal observation of fluorescence is well borne out by the observed spectra for Pr^{3+}, Nd^{3+}, Sm^{3+}, Eu^{3+}, Er^{3+}, and Tm^{3+} in LaF_3. If, in addition, one notes that the probability of radiative decay from higher excited states is enhanced because of the ν^3 dependence of the dipolar spontaneous emission probability and the larger number of possible terminal states,[49] semiquantitative estimates of the lifetimes and relative fluorescence intensities can be attempted.

The magnitude of W^{NR} and its dependence on energy gaps in Fig. 2 is not applicable to other crystals, however. The rates of phonon processes are a function of the modes and frequencies of vibrations which, in turn,

[46] The calculated radiative lifetime of $^4I_{13/2}$, which has the largest energy gap (≈ 6200 cm^{-1}) and is omitted from Fig. 1, is actually shorter than the observed τ. This discrepancy arises from and reflects the above uncertainties.

[47] If one assumes phonons of ≈ 350 cm^{-1} are dominant, then from Fig. 2, $W^{NR} \approx 2\times 10^5$ sec^{-1} for a five-phonon process (energy gap of 1750 cm^{-1}). Taking $W^{NR}(n \text{ phonons})/W^{NR}(n+1 \text{ phonons}) \sim 20$ and extrapolating yields a rate of 3×10^{10} sec^{-1} for a one-phonon transition. This would produce lifetime broadening of a crystal-field level at 350 cm^{-1} of ~ 1 cm^{-1}. At the other extreme, the estimated rate of a ten-phonon process bridging an energy gap of 3500 cm^{-1} would be ~ 0.1 sec^{-1} and hence possibly negligible compared to radiative probabilities. That this admittedly crude, order-of-magnitude numerology yields results which are not extraordinarily unreasonable (they are probably within one or two orders of magnitude of actual values) attests to the averaging out of details arising from interactions involving many different levels and vibrational modes.

[48] R. Orbach, Phys. Rev. **133**, A34 (1964).

[49] This is evident for $^2P_{3/2}$ and $^4D_{5/2}$ where, from Fig. 1, the radiative rates are larger than those of lower levels having comparable energy gaps.

are properties of the host lattice in which the ion is embedded. This dependence on host lattice is reflected in the reported[50] minimum energy gap required for the appearance of Er^{3+} fluorescence which ranges from $\approx$900 cm^{-1} in $LaCl_3$ to $\sim$4000 cm^{-1} in some glasses.

SUMMARY

Excited rare-earth ions in crystals relax in general by a combination of radiative and nonradiative processes. The present investigation has demonstrated that the individual rates of these processes and the quantum efficiencies for specific levels can be determined from measurements of excited-state lifetimes and calculated spontaneous emission probabilities. The latter are predominantly electric-dipole in nature for $LaF_3:Er^{3+}$ and were calculated from the phenomenological treatment of Judd and Ofelt and experimental oscillator strengths. To get truly quantitative results, calculations using crystal-field eigenstates are obviously needed. However, even though the use of intermediate coupled states, the assumption of equally populated crystalline Stark manifolds, neglect of J-state mixing, and the approximations inherent in the Judd–Ofelt theory limit the accuracy of the present results, they are, nevertheless, vaulable in explaining the relaxation and spectral properties. The rates of nonradiative transitions between J multiplets, obtained from comparison of measured lifetimes and total calculated radiative lifetimes, are found, as expected, to be very sensitive to the energy of the transition to the next-lower multiplet. These processes are attributed to multiphonon emission and appear to make significant contributions to the lifetimes of fluorescent states of rare earths in LaF_3 even for large transitions corresponding to the simultaneous emission of 5–6 phonons. A study of the dependence of the nonradiatives probabilities on the properties of the host lattice would be of interest to further the understanding of multiphonon processes.

ACKNOWLEDGMENTS

I wish to thank Mrs. Yvonne Leighton for recording the absorption spectra and for numerous calculations. The computer program for fitting the energy levels was developed by P. Nutter, and the assistance of Mrs. Marilyn Blodgett in its use and for other computations is very gratefully acknowledged.

[50] G. H. Dieke, in *Paramagnetic Resonance*, edited by W. Low (Academic Press Inc., New York, 1963), Vol. I, p. 237.

PHYSICAL REVIEW VOLUME 157, NUMBER 2 10 MAY 1967

Magnetic Resonance of Mn^{++} in PbS, PbSe, and PbTe†

JOE H. PIFER* ‡
Department of Physics and Materials Research Laboratory, University of Illinois, Urbana, Illinois

(Received 21 December 1966)

The paramagnetic resonance of Mn^{++} in various lead salts has been observed at 1.3 and 77°K. The spectrum shows hyperfine splitting, but no crystal-field splitting. The hyperfine constant of Mn^{++} in PbS, PbSe, and PbTe is 71.8, 67.6, and 61.2×10^{-4} cm^{-1}, respectively. An anomalous g shift of the hyperfine lines is attributed to the electronic equivalent of the Knight shift. Electronic inhomogeneity in PbSe results in two separate sets of hyperfine lines. It is suggested that the inhomogeneity is due to a clustering of lead vacancies. The spectrum of Eu^{++} in PbSe is also reported.

I. INTRODUCTION

THE paramagnetic resonance of manganese in a cubic environment has been studied in a very large variety of insulators and semiconductors.[1,2] It has also been seen in metals as a broad featureless line.[3] We report here the magnetic resonance of Mn^{++} in the degenerate semiconductors PbSe, PbS, and PbTe. In PbSe and PbTe (and probably PbS) we observe anomalies which we attribute to free-carrier effects. We have also observed the resonance of Eu^{++} in PbSe, and an unknown resonance at $g=2$ in all three materials.

II. SAMPLE PREPARATION AND APPARATUS

The single crystals were grown by a modified Bridgman technique, following the procedure described by Lawson.[4] The starting materials for the PbSe crystals were 99.999% pure ASARCO Pb and Se. In the PbS and PbTe crystals, 99.9% S and Te were used. All the samples used had 0.01% Mn added to the elements

† Supported by the U.S. Atomic Energy Commission under Contract No. AT(11-1)-1198, Report No. COO-1198-407.
* Texas Instruments Fellow.
‡ Present address: Department of Physics, Rutgers University, New Brunswick, New Jersey.
[1] G. W. Ludwig and H. H. Woodbury, in *Solid State Physics*, edited by F. Seitz and D. Turnbull (Academic Press Inc., New York, 1962), Vol. 13, p. 223.
[2] W. Low, in *Solid State Physics*, edited by F. Seitz and D. Turnbull (Academic Press Inc., New York, 1960), Vol. 2, Suppl., pp. 118–119.
[3] J. Owen, M. Browne, W. D. Knight, and C. Kittel, Phys. Rev. **102**, 1501 (1956).
[4] W. D. Lawson, J. Appl. Phys. **22**, 1444 (1951).